ARCHIVES OF ELECTRICAL ENGINEERING VOL. 67(2), pp. 307–320 (2018)

DOI 10.24425/119642

Fuzzy logic controller based maximum power point tracking technique for different configurations of partially shaded photovoltaic system

B. KRISHNA NAICK[1], K. CHATTERJEE[1], T.K. CHATTERJEE[2]

[1] *Departement of Electrical Engineering*
Indian Institute of Technology (Indian School of Mines)
Dhanbad, Jharkhand, India – 826004

[2] *Department of Mining Machinery Engineering*
Indian Institute Of Technology (Indian School of Mines)
Dhanbad, Jharkhand, India – 826004
e-mail: krishnalalitha.b@gmail.com

(Received: 04.03.2017, revised: 03.02.2018)

Abstract: A solar photovoltaic (PV) system has been emerging out as one of the greatest potential renewable energy sources and is contributing significantly in the energy sector. The PV system depends upon the solar irradiation and any changes in the incoming solar irradiation will affect badly on the output of the PV system. The solar irradiation is location specific and also the atmospheric conditions in the surroundings of the PV system contribute significantly to its performance. This paper presents the cumulative assessment of the four MPPT techniques during the partial shading conditions (PSCs) for different configurations of the PV array. The partial shading configurations like series-parallel, bridge link, total cross tied and honeycomb structure for an 8×4 PV array has been simulated to compare the maximum power point tracking (MPPT) techniques. The MPPT techniques like perturb and observe, incremental conductance, extremum seeking control and a fuzzy logic controller were implemented for different shading patterns. The results related to the maximum power tracked, tracking efficiency of each of the MPPT techniques were presented in order to assess the best MPPT technique and the best configuration of the PV array for yielding the maximum power during the PSCs.

Key words: partially shaded configuration, photovoltaic system, maximum power point tracking, fuzzy logic controller, tracking efficiency

1. Introduction

As a part of a drive to produce clean energy, most of the developing countries are opting the renewable energy sources like solar and wind energy to meet their power demand. From the

existing types of renewable energy sources, the source that will be suitable for the generation of power depends upon the different factors of the location. The solar energy is the best suitable for any location, as the solar irradiation will be available throughout the year. To harness energy from the solar irradiation, photovoltaic (PV) systems are widely used. The surrounding temperature and solar irradiation will greatly affect the PV system performance due to its nonlinear behaviour. The atmospheric conditions and the objects coming in between the irradiation and PV system will lead to the partial shading. The partial shading is considered to be one of the faulty conditions of the PV system. In addition to this, the different types of faulty conditions as mentioned in [1] are: a line-ground fault, line-line fault and open-circuit fault. The partial shading conditions will reduce the maximum power to be produced by the PV system.

To ensure the maximum power from the PV system at any environmental conditions, the maximum power point (MPP) tracking (MPPT) techniques in combination with a central DC-DC converter will be employed [2]. Under partial shading conditions (PSC), the PV module will behave as a load and the current produced by the other modules will be absorbed by the shaded module. To avoid this condition, the bypass diodes will be used in parallel with each of the PV modules. Due to these bypass diodes, the P-V characteristics will be having multiple MPP peaks in which there will be only one global peak [3, 4] and the task of the MPPT technique is to track the global peak. So many MPPT techniques are present in the literature for tracking an MPP in uniform and non-uniform conditions of solar irradiation.

The conventional MPPT techniques for PSCs are: a constant voltage controller, perturb & observe (P&O) and incremental conductance (INC) [5, 6]. The artificial intelligence (AI) based MPPT techniques for PSCs are: an artificial neural network (ANN) [7, 8] and fuzzy logic controller (FLC) [9, 10]. The bio-inspired optimization techniques based MPPT algorithms for PSCs are: a genetic algorithm (GA) [11], particle swarm optimization (PSO) [12], firefly (FF) [13], an artificial bee colony (ABC) [14], ant colony (AC) [15], cuckoo search [16] and grey wolf optimization [17]. Since, the partially shaded PV array will be having multiple peaks, the conventional MPPT techniques will progress towards only one of the nearest local peak and it will not progress further to reach the global peak which is considered to be the major disadvantage [3]. From the MPPT algorithms found in the literature, it has been observed that the authors try to explain the merits of their proposed algorithm when compared to the other algorithms and the proposed algorithms were explained only for a limited partial shading conditions. It has been also found that the manufacturers supplying the PV system are not implementing the newly proposed optimization based algorithms for tracking the MPP during the PSCs. The PSC is one of the most important and critical areas of operation of the PV system, as its output power reduces drastically. Hence, it is required to assess the performance of these MPPT techniques extensively for different PSCs and also to find out the best suitable configuration of a PV array during the PSCs from the operational point of view. For this purpose, the most popular MPPT techniques have been selected in addition to the typical shading patterns and the different configurations of the PV array.

In this paper, the MPPT techniques like P&O, INC, FLC and extremum seeking control (ESC) [18] were implemented on partially shaded PV arrays. The SP, BL, TCT and HCS are the configurations of the shaded PV modules considered to implement the MPPT techniques. An analysis in terms of a global maximum power point (GMPP), tracked by each technique, the voltage at the GMPP and the stability time for the above said PSCs have been presented.

An array of 8×4 modules has been considered for implementation. The rest of the paper has been organized in the following manner: – the modeling of the PV module has been explained in section 2; the implemented MPPT techniques has been discussed in section 3; the simulation results were explained in section 4.

2. Modeling of PV module

The electrical equivalent model of a solar PV module may be represented by using a single diode or a two diode equivalent circuit, of which the single diode model has been considered in the present work because of its simplicity and higher efficiency. The equivalent circuit is shown in Fig. 1.

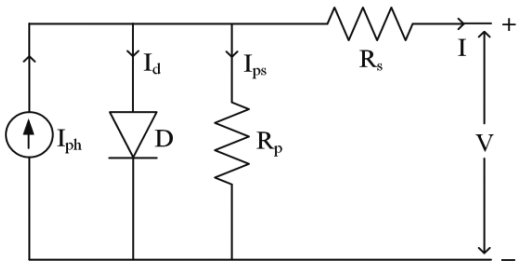

Fig. 1. Single diode equivalent circuit

The output current I of the PV module [19] is expressed by (1).

$$I = I_{ph} - I_d - I_{ps}\,, \tag{1}$$

whereas I_{ph} is the current due to incident solar irradiation and I_d is the saturation current and I_{ps} is the current flowing through the shunt resistance R_{sh}.

The current due to incident solar irradiation is represented by (2).

$$I_{ph} = (I_{sc,n} + K_I\, d\, T)\frac{G}{G_n}\,. \tag{2}$$

$I_{sc,n}$ is the current produced at nominal conditions of 1000 W/m^2 and 25°C. K_I is the short circuit current/temperature coefficient. The difference between the operating (T) and nominal temperature (T_n) in Kelvin is represented by dT, which is expressed as $dT = T - T_n$. G and G_n in W/m^2 are the incident and nominal solar irradiation. The saturation current I_d is expressed by (3).

$$I_d = I_0\left[\exp\left(\frac{V + IR_S}{V_t a}\right) - 1\right]. \tag{3}$$

I_0 is the diode saturation current. V and I are the output voltage and current of the PV module and R_S in Ω is the series resistance. "a" is the diode ideality factor and its value lies in the range of 1 to 2. V_t is the thermal voltage and is expressed as $V_t = N_S kT/q$. The number of cells connected in series in the PV module is represented by N_S, k is the Boltzmann constant $(1.3806503 \times 10^{-23}$ J/K) and q is the charge of the electron $(1.60217646 \times 10^{-19}$ C).

The diode saturation current I_0 is expressed by (4).

$$I_0 = I_{0,n}\left(\frac{T_n}{T}\right)^3 \exp\left[\frac{qE_g}{ak}\left(\frac{1}{T_n}-\frac{1}{T}\right)\right], \tag{4}$$

whereas E_g is the bandgap energy of the $p-n$ junction material used in a solar cell. $I_{0,n}$ is the nominal saturation current expressed as in (5).

$$I_{0,n} = \frac{I_{sc,n}}{\exp\left(\dfrac{V_{oc,n}}{aV_{t,n}}\right)-1}. \tag{5}$$

$V_{oc,n}$ and $V_{t,n}$ are the open circuit and thermal voltage at nominal conditions. The shunt current is represented by Equation (6).

$$I_{ps} = \frac{V+IR_S}{R_P}. \tag{6}$$

Substituting Equations (3) and (6) into (1), the expression for the output current of the PV module is given by (7).

$$I = I_{ph} - I_0\left[\exp\left(\frac{V+IR_S}{V_t a}\right)-1\right] - \frac{V+IR_S}{R_P}. \tag{7}$$

3. Maximum power point tracking techniques

At any environmental conditions, the maximum energy from the PV system may be yielded by employing the MPPT controller. The MPPT controller will have a suitable DC-DC converter and the MPPT technique. The purpose of the MPPT controller is to drive the PV array at an MPP by calculating the suitable duty cycle and to control the switch present in the converter, so that, the input side resistance (resistance of the PV array) of the converter should be equal to the output side resistance (resistance of the load) for extracting the maximum energy according to the maximum power transfer theorem. To increase or decrease the output voltage of the PV array, a suitable DC-DC converter may be selected from the existing converter topologies. The topologies like buck, boost, buck-boost and cuk were found in the literature. In the present work, the boost converter has been implemented, as it is suitable to generate higher output voltage for interfacing the PV system with grid or high power loads. The relationship between the resistance of the PV array (R_{pv}), load resistance (R_{load}) and duty cycle d_o is given by (8) [20].

$$R_{pv} = R_{\text{load}}(1-d_o)^2. \tag{8}$$

The MPPT techniques implemented for changing the duty cycle of a boost converter have been discussed in this section.

3.1. P&O method:

It is one of the conventional MPPT technique and is implemented as in [21]. The voltage (V) and current (I) of a PV array at present (c^{th}) and previous positions ($(c-1)^{\text{th}}$) will be measured

and power at these positions will be calculated. Whenever, the power of the present position $P(c)$ is greater than the previous position $P(c-1)$ and the voltage at the present position $V(c)$ is greater than the voltage at the previous positon $V(c-1)$, then the tracking of power will be continued on the left side of the MPP by enhancing the duty cycle to a small value only. Or else, when $P(c)$ will be less than the $P(c-1)$ and $V(c)$ is greater than $V(c-1)$, then the tracking will be continued on the right side of the MPP by decreasing the duty cycle to a small value. The tracking speed depends upon the step value of the duty cycle. It will be faster with a larger step value and slower with a smaller step value. The disadvantage is that with the increase in perturbation value, there will be huge oscillations at the MPP, power loss and also impossibility to track the MPP under fast changing environmental conditions. The advantage is that, it is having less complexity.

3.2. INC method:

The INC algorithm directly depends upon the variation of power only. At the MPP, the slope of the P-V curve or the derivative of power with respect to voltage will be zero, whereas it is positive on its left side and negative on its right side [22]. The expression to operate INC at the optimal value of the MPP is given by (9) and (10) [6].

$$\frac{\mathrm{d}P_A}{\mathrm{d}V_A} = \frac{\mathrm{d}(V_A I_A)}{\mathrm{d}V_A} = I_A + V_A \frac{\mathrm{d}I_A}{\mathrm{d}V_A} = 0, \tag{9}$$

$$\frac{I_A}{V_A} = \frac{\mathrm{d}I_A}{\mathrm{d}V_A}. \tag{10}$$

At the same time, the conditions that should be satisfied to operate the INC at the MPP value is expressed by (11) and (12).

$$\frac{\mathrm{d}I_A}{\mathrm{d}V_A} = \frac{I_A}{V_A}, \tag{11}$$

$$\frac{\mathrm{d}I_A}{\mathrm{d}V_A} = -\frac{I_A}{V_A}. \tag{12}$$

The change in voltage and current will be calculated by measuring the voltage V and current I at the present position (c) and previous position $(c-1)$. The change in the voltage $\mathrm{d}V_A$ is expressed by $V_A(c) - V_A(c-1)$, whereas, the change in the current $\mathrm{d}I_A$ is expressed by $I_A(c) - I_A(c-1)$. The duty cycle may be enhanced or decreased by a small value according to the following conditions.

- If the value of $\mathrm{d}V_A$ and $\mathrm{d}I_A$ is zero, then the duty cycle will be maintained constant.
- If the value of $\mathrm{d}V_A$ is zero and $\mathrm{d}I_A$ is not equal to zero, then the $\mathrm{d}I_A$ will be checked to have a value greater or less than that of zero. If $\mathrm{d}I_A$ has value greater than zero, then the duty cycle will be increased by a small value or else it will be decreased by a small value.
- If $\mathrm{d}V_A$ is not equal to zero, then the condition in (10) will be checked. The current duty cycle will remain unchanged, only when the condition in (10) is satisfied.
- If the condition in (10) is not satisfied, then the condition represented in (11) will be checked. If it is satisfied, then the duty cycle will be decreased by a small value or else, the duty cycle will be increased by a small value.

The merit of the INC method is that it will track the optimal value of an MPP at any environmental conditions, whereas, the demerit is its complexity and the effect of size of incremental value in tracking MPP.

3.3. ESC method:

The ESC method is used to find the extreme (either peak or base) points in a geographical area. The flow diagram as in [23] is implemented in this model. The ESC consists of a gradient detector (GD), an integrator and a perturbation based sinusoidal signal (also called as dither signal) with its amplitude (a) and frequency (ω). The GD consists of a high pass filter (HPF) and low pass filter (LPF) with frequencies ω_h and ω_l. The output power of a PV array is fed as input signal to the GD, in which, it is fed to the HPF for removing the DC component present in the signal. Based upon the resultant signal obtained from the high pass filter, it may be estimated that whether the duty cycle 'd_o' fed to the DC-DC converter is an optimal value or not for tracking the MPP.

The resultant signal will be multiplied with the perturbation signal, which will be acting as a demodulating signal. If the resultant signal from the high pass filter is in phase with the perturbation sinusoidal signal, then it indicates that the fed duty cycle d_o is greater than the optimal value d_o^*. Similarly, if the resultant signal is out of phase with respect to perturbation signal, then it indicates that the fed duty cycle d_o is less than the optimal value d_o^*. If the frequency of the resultant signal is twice the frequency of a sinusoidal signal, then it indicates that the fed duty cycle d_o is equal to the optimal value d_o^* and the MPP is tracked. Further, if any DC components present in the demodulating signal will be removed by the LPF. The signal obtained from the GD is known as the gradient of the input signal $\bar{g}$ and will be fed as an input to the integrator for vanishing the gradient. The gain in the integrator will improve the transient performance of the gradient signal [24]. The output signal of the integrator is the duty cycle $\bar{d}$ and it will be further added with the perturbation signal to obtain the duty cycle d_o. In order to obtain the best optimal value of a duty cycle, the frequencies ω, ω_h and ω_l should be in the order of $\omega_h < \omega$ and $\omega_l < \omega$ [23].

3.4. FLC method:

An FLC is a simple and nonlinear controller, which is based upon the linguistic rules. The mathematical model and technical specifications of the plant or system is not required in an FLC based system [25]. Mamdani (M) and Tagachi-Sukeno (T-S) are the two design approaches available in the FLC. A Mamdani based FLC is most popular and the same is implemented in this paper. Fuzzification, rule interference and defuzzification are the three stages of the FLC. The process of converting the input crisp values into fuzzy values via membership functions is called fuzzification. Triangular, Gaussian and Trapezoidal are the different types of existing fuzzy membership functions, of which, the most popular is the triangular membership function. In a rule-base inference system, a total of 25 rules has been implemented by combining the input and output membership functions as shown in Table 1. The concept of "if-then" is used for framing the rules. Defuzzification is the process of converting the fuzzy membership functions into output crisp values for controlling the plant.

The implemented defuzzification method is the centre of area (COA) method and in this method, the output is calculated by using (13).

$$\Delta D(k) = \frac{\sum_{j=1}^{n} \mu(\Delta D_j(k)) X \Delta D_j(k)}{\sum_{j=1}^{n} \mu(\Delta D_j(k))}. \tag{13}$$

Table 1. Rules of FLC

		der				
		NE	NF	ZR	PF	PE
er	NE	NE	NE	NF	NF	ZR
	NF	NE	NF	NF	ZR	PF
	ZR	NF	NF	ZR	PF	PF
	PF	NF	ZR	PF	PF	PE
	PE	ZR	PF	PF	PE	PE

The inputs to the FLC are the error '*er*' and the change in error '*der*' and are given by the Equations (14) and (15), whereas the output is the duty cycle 'd_o'.

$$er = \frac{\mathrm{d}P}{\mathrm{d}V}, \tag{14}$$

$$der = \frac{\mathrm{d}P}{\mathrm{d}V}(k) - \frac{\mathrm{d}P}{\mathrm{d}V}(k-1). \tag{15}$$

whereas '*er*' is the differentiation of power with respect to voltage and '*der*' is the difference in errors at the k^{th} and $(k-1)^{\text{th}}$ position. The membership functions of the '*er*', '*der*' and 'd_o' of the implemented FLC is to track an MPP in a partially shaded PV system.

4. Implementation and results

A PV array with 8 number of series connected modules and 4 parallel strings having an output power of 6 kW at nominal irradiation conditions has been considered. The parameters of a KC200GT PV module [19] as given in Table 2 has been selected. The boost converter, suitable for high voltage applications has been considered to operate the PV array at an MPP. The value of the inductance and the DC link capacitance of a boost converter are 7.272 mH and 500 μF. A comparative analysis based upon the tracking of an MPP, tracking efficiency and tracking time of different MPPT techniques is carried out for different partially shaded configurations using a MATLAB/Simulink platform. The configurations like series-parallel (SP), bridge-link (BL), total cross tied (TCT) and honeycomb structure (HCS) were implemented for the selected shading patterns [26]. To implement the shading patterns, the modules of an 8×4 PV array have been divided into four parts, i.e. a lower end, lower middle, upper middle and upper end with each containing 2×4 modules. The selected shading patterns have been represented as P1, P2, P3 and P4 as given in Table 3. In the pattern P1, an irradiation of 1000 W/m^2 is applied to the upper end, 750 W/m^2 to the upper middle, 500 W/m^2 to the lower middle and 250 W/m^2 to the lower end of the PV array. The same strategy is followed while applying the remaining three patterns P2, P3 and P4.

The MPPT techniques like P&O, INC, ESC and FLC were implemented in the above said configurations of the PV array. In P&O and INC methods, a perturbation value (also called an

Table 2. KC200GT Parameters

Open circuit voltage	32.9 V
Short circuit current	8.21 A
Diode ideality factor	1.3
Short circuit current temperature coefficient	0.0032 A/K
Series resistance	0.221 Ω
Shunt resistance	415.405 Ω
Number of cells in a module	54

Table 3. Implemented shading patterns along with GMPP

Shading patterns in W/m^2.					**GMPP (W)**
P1	1000	750	500	250	2586
P2	800	600	400	200	2041
P3	600	500	400	300	2046
P4	750	500	200	100	1602

incremental value in INC) of 0.01 has been applied to perturb the duty cycle 'd' in the increasing or decreasing direction of the MPP. In the ESC, the frequencies of a perturbation signal, LPF and HPF are 110, 60 and 100 rad/s, which also satisfies the given condition $\omega_h < \omega$ and $\omega_l < \omega$.

For the selected shading patterns, the I-V and P-V characteristics of the PV array are shown in Fig. 2 and Fig. 3. From Fig. 3, it may be observed that for each pattern, the P-V characteristics are having different MPPs, which are also called the local peaks. Of these local peaks, the peak, which will have the higher MPP value is called the global peak and needs to be tracked by the above MPPT techniques. For the selected patterns, the value of the global maximum power point (GMPP) is given in Table 3. In order to assess the MPPT techniques, the shading patterns were

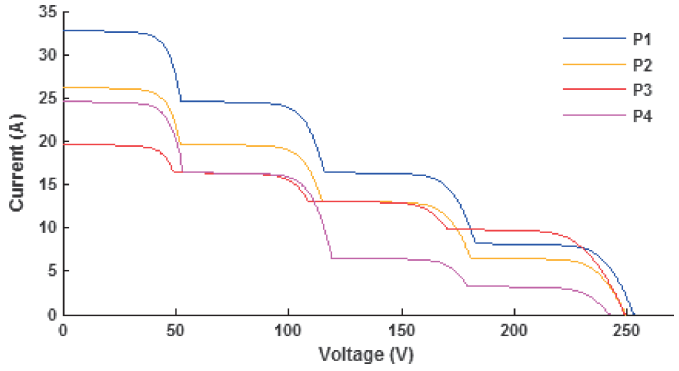

Fig. 2. I-V characteristics

applied to SP, BL, TCT and HCS configurations. The pattern P1 has been applied to the PV array from 0 to 1 s, P2 from 1 to 2 s, P3 from 2 to 3 s and P4 from 3 to 4 s. The GMPP tracked by the MPPT techniques are shown in Fig. 4, Fig. 5, Fig. 6 and Fig. 7. From Fig. 4 and Fig. 5, it may

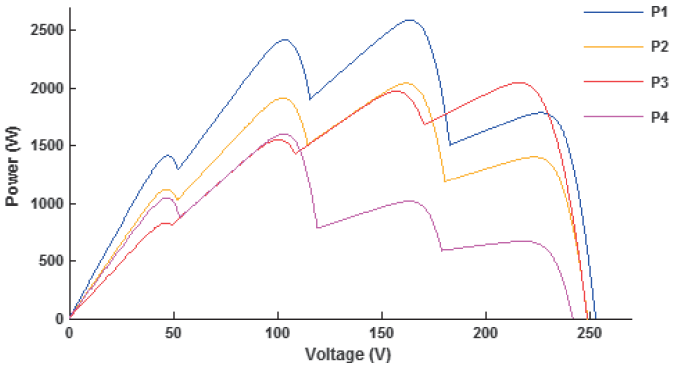

Fig. 3. P-V characteristics

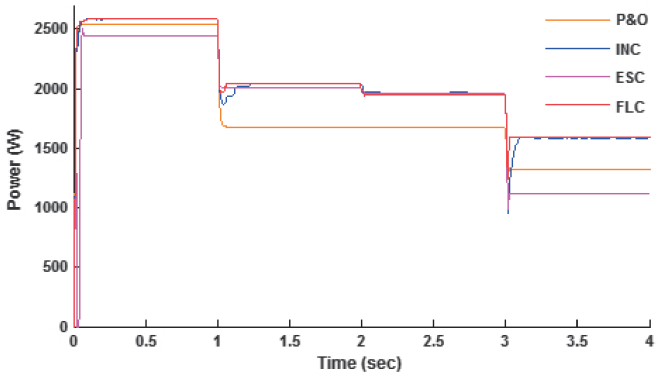

Fig. 4. Power comparison in SP configuration

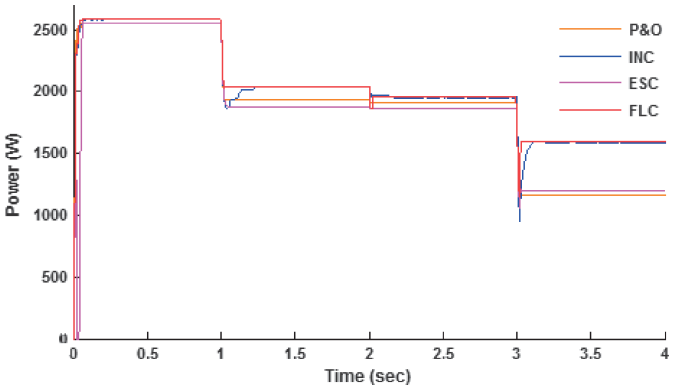

Fig. 5. Power comparison in BL configuration

be observed that in SP and BL configurations, whenever the shading pattern changes, the GMPP tracked by the P&O method has a lower value when compared to other methods. Whereas in TCT and HCS configurations, the P&O method is tracking the GMPP value almost equal to the value tracked by other techniques, as shown in Fig. 6 and Fig. 7.

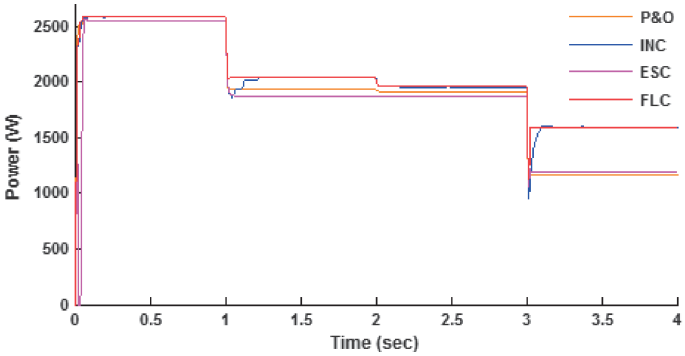

Fig. 6. Power comparison in TCT configuration

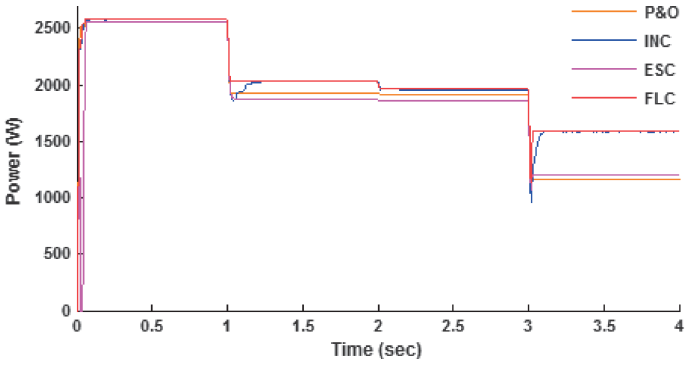

Fig. 7. Power comparison in HCS configuration

From Fig. 4, Fig. 5, Fig. 6 and Fig. 7, it has been observed that the GMPP value tracked by the ESC method also has a lower value when compared to other techniques. In addition to this, it has been also found that the GMPP tracked by ESC for the fourth shading pattern (from 3 to 4 s) is much lower. The GMPP tracked by the INC and FLC methods are having equal values for the first two patterns, whereas, the performance of the FLC is better in tracking the GMPP value for the remaining two patterns as shown in Fig. 4, Fig. 5, Fig. 6 and Fig. 7. The GMPP value tracked by the above mentioned MPPT techniques are presented in Table 4. From Table 4, it may be observed that the FLC tracks the optimal GMPP value for each of the shading patterns in all the configurations of the PV array.

The time taken to track the stable GMPP value by the MPPT techniques is presented in Table 5. From Fig. 4, Fig. 5, Fig. 6, Fig. 7 and Table 5, it may be observed that the time taken

Table 4. GMPP tracked by the MPPT and tracking efficiency

Shading Pattern		P1	P2	P3	P4
GMPP obtained from P-V characteristics (W)		2586	2041	2046	1602
The maximum power in Watts, tracked by each MPPT method and tracking efficiency in %					
SP	P&O	2546, 98.45	1678, 82.21	1671, 81.67	1315, 82.08
	INC	**2586, 100**	**2041, 100**	**1952, 95.4**	1585, 98.93
	ESC	2445, 94.54	2003, 98.13	1962, 95.89	1114, 69.53
	FLC	**2586, 100**	**2041, 100**	**1952, 95.4**	**1592, 99.37**
BL	P&O	2584, 99.92	1932, 94.65	1914, 93.54	1161, 72.47
	INC	**2586, 100**	**2041, 100**	1951, 95.35	1585, 98.93
	ESC	2553, 98.72	1874, 91.81	1863, 91.05	1196, 74.65
	FLC	**2586, 100**	**2041, 100**	**1959, 95.74**	**1589, 99.18**
TCT	P&O	2584, 99.92	1932, 94.65	1914, 93.54	1161, 72.47
	INC	**2586, 100**	**2041, 100**	1952, 95.4	1585, 98.93
	ESC	2553, 98.72	1874, 91.81	1863, 91.05	1196, 74.65
	FLC	**2586, 100**	**2041, 100**	**1965, 96.04**	**1593, 99.43**
HCS	P&O	2584, 99.92	1932, 94.65	1914, 93.54	1161, 72.47
	INC	**2586, 100**	**2041, 100**	1953, 95.45	1586, 99
	ESC	2553, 98.72	1874, 91.86	1854, 90.61	1196, 74.65
	FLC	**2586, 100**	**2041, 100**	**1965, 96.04**	**1595, 99.56**

by the FLC method is much shorter when compared to the other techniques for each pattern and the shading configuration of a PV array. The time taken by the P&O and ESC methods is also much shorter, but a low value of the GMPP was tracked when compared to the INC and FLC techniques. Though the INC method used to track the GMPP value equals to that of the FLC, but the tracking time is longer, the same may be observed in Table 5.

The tracking efficiency exhibited by each technique has been presented in Table 4. In all the four configurations of the PV array, the tracking efficiency of the INC and FLC techniques are 100% for patterns P1 and P2, whereas, it has been in the range of 95–96% for P3 and 98–99.6% for P4. The tacking efficiency of the ESC method is above 90% for the patterns P1, P2 and P3 and it is in the range of 72–75% for P4. Similarly, the tracking efficiency of the P&O method is above 90% for the patterns P1, P2 and P3 in the BL, TCT and HCS configurations and it is in the range of 72–75% for P4. In the SP configuration, the tracking efficiency is above 98% for P1 and it is in the range of 82–85% for P2, P3 and P4.

Hence, from these observations, it may be concluded that out of the above said four MPPT algorithms that can be implemented by the manufacturers during the PV installation, the FLC

Table 5. Tracking time

Tracking time in seconds					
MPPT techniques and Shading Pattern		P1	P2	P3	P4
SP	P&O	0.097	0.072	0.033	0.035
	INC	0.222	0.245	0.163	0.21
	ESC	**0.088**	0.067	0.034	0.038
	FLC	0.11	**0.058**	**0.056**	**0.039**
BL	P&O	0.074	0.035	0.035	0.034
	INC	0.222	0.245	0.172	0.211
	ESC	0.08	0.073	0.027	0.039
	FLC	**0.067**	**0.029**	**0.024**	**0.027**
TCT	P&O	0.073	0.036	0.034	0.04
	INC	0.222	0.245	0.163	0.212
	ESC	0.09	0.073	0.027	0.045
	FLC	**0.065**	**0.016**	**0.017**	**0.031**
HCS	P&O	0.088	0.037	0.034	0.04
	INC	0.23	0.249	0.159	0.207
	ESC	0.087	0.073	0.047	0.039
	FLC	**0.065**	**0.016**	**0.016**	**0.029**

method is quite efficient in tracking the GMPP value with less tracking time during the PSCs. Also, it may be observed that to maximize the output power during the PSCs, the TCT configuration of the PV array generates more output power when compared to the remaining three configurations.

5. Conclusion

In this paper, an 8×4 PV array of 6 kW under nominal irradiation conditions has been simulated to analyze the performance of P&O, INC, ESC and FLC based MPPT methods during the PSCs that will be helpful for installation of the PV system. Also, the assessment was carried out to find the best suitable configuration of the PV array during the PSCs from the configurations like SP, BL, TCT and HCS. The 8×4 PV array has been divided into 4 sections of 2×4 structure to apply the rapidly changing shading patterns P1, P2, P3 and P4 for a period of 1 second each. From the results, it has been found that the FLC method is quite efficient in tracking the GMPP value with less tracking time. Though the INC method is tracking the GMPP value equivalent

to that of FLC but the tracking time is longer. The P&O and ESC methods are not able to track the GMPP value with the change in the shading patterns. Also, it has been found that the TCT configuration produces maximum power during the partially shaded conditions.

References

[1] Hariharan R., Chakkarapani M., Ilango G.S., Nagamani C., *A Method to Detect Photovoltaic Array Faults and Partial Shading in PV Systems*, IEEE Journal of Photovoltaics, vol. 6, no. 5, pp. 1278–1285 (2016).

[2] Luo H., Wen H., Li X., Jiang L., Hu Y., *Synchronous buck converter based low-cost and high-efficiency sub-module DMPPT PV system under partial shading conditions*, Energy Conversion and Management, vol. 126, pp. 473–487 (2016).

[3] Lian K.L., Jhang J.H., Tian I.S., *A Maximum Power Point Tracking Method Based on Perturb-and-Observe Combined With Particle Swarm Optimization*, IEEE Journal of Photovoltaics, vol. 4, no. 2, pp. 626–633 (2014).

[4] Ghasemi M.A., Forushani H.M., Parniani M., *Partial Shading Detection and Smooth Maximum Power Point Tracking of PV Arrays Under PSC*, IEEE Transactions on Power Electronics, vol. 31, no. 9, pp. 6281–6292 (2016).

[5] Gupta A., Chauhan Y.K., Pachauri R.K., *A comparative investigation of maximum power point tracking methods for solar PV system*, Solar Energy, vol. 136, pp. 236–253 (2016).

[6] Ishaque K., Salam Z., Lauss G., *The performance of perturb and observe and incremental conductance maximum power point tracking method under dynamic weather conditions*, Applied Energy, vol. 119, pp. 228–236 (2014).

[7] Mekki H., Mellit A., Salhi H., *Artificial neural network-based modelling and fault detection of partial shaded photovoltaic modules*, Simulation Modelling Practice and Theory, vol. 67, pp. 1–13 (2016).

[8] Elobaid L.M., Abdelsalam A.K., Zakzouk E.E., *Artificial neural network-based photovoltaic maximum power point tracking techniques: a survey*, IET Renewable Power Generation, vol. 9, no. 8, pp. 1043–1063 (2015).

[9] Alajmi B.N., Ahmed K.H., Finney S J., Williams B.W., *A Maximum Power Point Tracking Technique for Partially Shaded Photovoltaic Systems in Microgrids*, IEEE Transactions on Industrial Electronics, vol. 60, no. 4, pp. 1596–1606 (2013).

[10] Sekhar P.C., Mishra S., *Takagi–Sugeno fuzzy-based incremental conductance algorithm for maximum power point tracking of a photovoltaic generating system*, IET Renewable Power Generation, vol. 8, no. 8, pp. 900–914 (2014).

[11] Daraban S., Petreus D., Morel C., *A novel global MPPT based on genetic algorithms for photovoltaic systems under the influence of partial shading*, Proceedings of the 39th Annual Conference of the IEEE Industrial Electronics Society, pp. 1490–1495, 10-13 November 2013.

[12] Ishaque K., Salam Z., *A Deterministic Particle Swarm Optimization Maximum Power Point Tracker for Photovoltaic System Under Partial Shading Condition*, IEEE Transactions on Industrial Electronics, vol. 60, no. 8, pp. 3195–3206 (2013).

[13] Sundareswaran K., Peddapati S., Palani S., *MPPT of PV Systems Under Partial Shaded Conditions Through a Colony of Flashing Fireflies*, IEEE Transactions on Energy Conversion, vol. 29, no. 2, pp. 463–472 (2014).

[14] Sundareswaran K., Sankar P., Nayak P.S.R., Simon S.P., Palani S., *Enhanced Energy Output From a PV System Under Partial Shaded Conditions Through Artificial Bee Colony*, IEEE Transactions on Sustainable Energy, vol. 6, no. 1, pp. 198–209 (2015).

[15] Sundareswaran K., Vigneshkumar V., Sankar P., Simon S.P., Nayak P.S.R., Palani S., *Development of an Improved P&O Algorithm Assisted Through a Colony of Foraging Ants for MPPT in PV System*, IEEE Transactions on Industrial Informatics, vol. 12, no. 1, pp. 187–200 (2016).

[16] Ahmed J., Salam Z., *A Maximum Power Point Tracking (MPPT) for PV system using Cuckoo Search with partial shading capability*, Applied Energy, vol. 119, pp. 118–130 (2014).

[17] Mohanty S., Subudhi B., Ray P.K., *A New MPPT Design Using Grey Wolf Optimization Technique for Photovoltaic System Under Partial Shading Conditions*, IEEE Transactions on Sustainable Energy, vol. 7, no. 1, pp. 181–188 (2016).

[18] Leyva R., Alonso C., Queinnec I., Pastor A.C., Lagrange D., Salamero L.M., *MPPT of Photovoltaic Systems using Extremum–Seeking Control*, IEEE Transactions on Aerospace and Electronic Systems, vol. 42, no. 1, pp. 249–258 (2006).

[19] Villalva M.G., Gazoli J.R., Filho E.R., *Comprehensive Approach to Modeling and Simulation of Photovoltaic Arrays*, IEEE Transactions on Power Electronics, vol. 24, no. 5, pp. 1198–1208 (2009).

[20] Başoğlu M.E., Çakır B., *Comparisons of MPPT performances of isolated and non-isolated DC–DC converters by using a new approach*, Renewable and Sustainable Energy Reviews, vol. 60, pp. 1100–1113 (2016).

[21] Femia N., Petrone G., Spagnuolo G., Vitelli M., *Optimization of Perturb and Observe Maximum Power Point Tracking Method*, IEEE Transactions on Power Electronics, vol. 20, no. 4, pp. 963–973 (2005).

[22] Sivakumar P., Kader A.A., Kaliavaradhan Y., Arutchelvi M., *Analysis and enhancement of PV efficiency with incremental conductance MPPT technique under non-linear loading conditions*, Renewable Energy, vol. 81, pp. 543–550 (2015).

[23] Malek H., Chen Y.Q., *Fractional Order Extremum Seeking Control: Performance and Stability Analysis*, IEEE/ASME Transactions on Mechatronics, vol. 21, no. 3, pp. 1620–1628 (2016).

[24] Li X., Li Y., Seem J.E., Lei P., *Detection of Internal Resistance Change for Photovoltaic Arrays Using Extremum-Seeking Control MPPT Signals*, IEEE Transactions on Control Systems Technology, vol. 24, no. 1, pp. 325–333 (2016).

[25] Seyedmahmoudian M., Horan B., Soon T.K., Rahmani R., Oo A.M.T., Mekhilef S., Stojcevski A., *State of the art artificial intelligence-based MPPT techniques for mitigating partial shading effects on PV systems – A review*, Renewable and Sustainable Energy Reviews, vol. 64, pp. 435–455 (2016).

[26] Ishaque K., Salam Z., Taheri H., Syafaruddin, *Modeling and simulation of photovoltaic (PV) system during partial shading based on a two-diode model*, Simulation Modelling Practice and Theory, vol. 19, pp. 1613–1626 (2011).